

See discussions, stats, and author profiles for this publication at: <https://www.researchgate.net/publication/239943070>

Spectroscopic characterization of copper(I) binding to apo and metal-reconstituted zinc finger peptides

ARTICLE *in* EUROPEAN JOURNAL OF BIOCHEMISTRY · JUNE 2013

Impact Factor: 2.54 · DOI: 10.1007/s00775-013-1012-6 · Source: PubMed

CITATIONS

2

READS

26

4 AUTHORS, INCLUDING:



[Korin E Wheeler](#)

Santa Clara University

13 PUBLICATIONS 261 CITATIONS

SEE PROFILE

Spectroscopic characterization of copper(I) binding to apo and metal-reconstituted zinc finger peptides

Reginald T. Doku, Grace Park, Korin E. Wheeler & Kathryn E. Splan

JBIC Journal of Biological Inorganic Chemistry

ISSN 0949-8257

J Biol Inorg Chem

DOI 10.1007/s00775-013-1012-6



Your article is protected by copyright and all rights are held exclusively by SBIC. This e-offprint is for personal use only and shall not be self-archived in electronic repositories. If you wish to self-archive your article, please use the accepted manuscript version for posting on your own website. You may further deposit the accepted manuscript version in any repository, provided it is only made publicly available 12 months after official publication or later and provided acknowledgement is given to the original source of publication and a link is inserted to the published article on Springer's website. The link must be accompanied by the following text: "The final publication is available at link.springer.com".

Spectroscopic characterization of copper(I) binding to apo and metal-reconstituted zinc finger peptides

Reginald T. Doku · Grace Park · Korin E. Wheeler · Kathryn E. Splan

Received: 28 March 2013 / Accepted: 29 May 2013
© SBIC 2013

Abstract Cu(I) exhibits high affinity for thiolate ligands, suggesting that thiol-rich zinc or iron binding sites may be subject to disruption during copper stress conditions. Zinc fingers constitute a large class of metalloproteins that use a combination of cysteine and histidine residues that bind Zn(II) as a structural element. Despite the shared preference of both copper and zinc for thiolate and amine coordination, the susceptibility of zinc finger domains toward copper substitution is not well studied. We report spectroscopic studies that characterize the Cu(I) binding properties of the zinc finger consensus peptides CP-CCHH, CP-CCHC, and CP-CCCC and the C-terminal zinc finger domain of HIV-1 nucleocapsid protein p7 (NCp7_C). Cu(I) binds to both the apo-peptides and the Co(II)-substituted peptides, and the stoichiometry of Cu(I) binding is dependent on the number of cysteine thiols at the metal binding site. Fluorescence studies of the Zn(II)–NCp7_C complex indicate that Cu(I) also effectively competes with Zn(II) at the metal binding site, despite the high affinity of Zn(II) for the CCHC binding motif. Circular dichroism studies on both CP-CCHC and NCp7_C show that the conformations of the Cu(I)-bound complexes differ substantially from those of the Zn(II) species, implying that Cu(I) substitution is likely to impact zinc finger function.

These results show that for the peptides studied here, Cu(I) is the thermodynamically favored metal despite the known high Zn(II) affinity of zinc finger domains, suggesting that Cu(I)-substituted zinc finger domains might be relevant in the context of both copper toxicity mechanisms and copper-responsive transcription factors.

Keywords Zinc fingers · Copper binding peptides · Electronic absorption spectroscopy · Metal ion toxicity

Abbreviations

BCA	Bicinchoninate
CD	Circular dichroism
DTNB	5,5'-Dithiobis(2-nitrobenzoic acid)
NCp7	Nucleocapsid protein p7 of human immunodeficiency virus type 1
NCp7_C	C-terminal zinc finger domain of NCp7
ZF	Zinc finger

Introduction

Eukaryotic organisms require copper ions for several essential functions, including oxidative phosphorylation, collagen formation, melanin production, and antioxidant activity. At elevated levels, however, copper is toxic to all cells, and both prokaryotic and eukaryotic species feature complex pathways to maintain copper homeostasis [1–3]. The mechanisms by which copper damages or kills cells are not fully known. Copper toxicity may be attributed, in part, to reactive oxygen species generated via Fenton chemistry that then react with DNA, proteins, and lipids, resulting in oxidative biomolecule damage [4]. However, a

Electronic supplementary material The online version of this article (doi:10.1007/s00775-013-1012-6) contains supplementary material, which is available to authorized users.

R. T. Doku · K. E. Splan (✉)
Department of Chemistry, Macalester College,
1600 Grand Avenue, Saint Paul, MN 55105, USA
e-mail: splank@macalester.edu

G. Park · K. E. Wheeler
Department of Chemistry and Biochemistry, Santa Clara
University, Santa Clara, CA 95053, USA

recent study showed that addition of copper ions to *Escherichia coli* cells decreased the rate at which H_2O_2 damaged DNA, challenging the notion that reactive oxygen species produced from copper-mediated processes are primarily responsible for copper toxicity [5]. A thorough mechanistic understanding of copper toxicity is of great medicinal interest, since several neurodegenerative diseases are associated with elevated copper levels and misregulated copper homeostasis [6–8].

The impact of copper ions on metalloprotein structure and function is not well understood and must also be considered in the context of copper toxicity. Cu(I), the predominant form of copper under the reducing conditions found in cells, is highly thiophilic, and many cellular copper-binding proteins use multiple cysteine and methionine residues for copper coordination. Recently, copper was shown to damage the iron–sulfur clusters of isopropylmalate dehydratase of *E. coli* both in vitro and in vivo in the absence of oxygen, suggesting that endogenous metal ion displacement at thiol-based binding sites by copper is a possible mechanism for copper toxicity [9]. Similarly, mutants of *Synechocystis* PCC 6803 lacking genes for both the copper chaperone Atx1 and glutathione synthetase exhibit hypersensitivity to elevated copper levels attributed to copper mislocation at both iron–sulfur clusters and the thiol-rich exchangeable zinc site of the metallosensor Zur [10]. The same report also shows that, in vitro, copper inhibits the mechanism of zinc sensing by Zur, but not by the zinc sensor ZiaR, implying that the susceptibility of zinc binding sites toward copper substitution is not universal.

Other plausible targets for copper ion toxicity are the zinc fingers (ZF), a large class of metalloproteins that bind Zn(II) via cysteine and histidine ligands in a tetrahedral geometry [11, 12]. Although ZFs were initially characterized as DNA-binding transcription factors, the term “zinc finger” (ZF) is often used to describe any compact domain stabilized by a zinc ion [13]. As defined, ZFs exhibit many functions, including DNA recognition, RNA packaging, regulation of apoptosis, and protein ubiquitination [14]. This functional diversity is reflected in the range of structural motifs identified to date, which have been classified into seven specific groups according to the domain fold [13]. A recent bioinformatics study estimates that zinc-binding proteins constitute 10 % of the human proteome, with ZF being the predominant class [15].

Despite the preferred Zn(II) coordination of ZFs, other metals with moderate to high affinity for thiolate and nitrogen ligands also bind to ZF domains, including Fe(II) [16, 17], Cd(II) [18, 19], Ni(II) [17, 20], and Co(II) [21–23]. Structural and quantitative binding studies also reveal that both Pb(II) [24, 25] and Au(I) [26, 27] compete directly with Zn(II) for thiolate-rich coordination sites,

resulting in a loss of protein function and providing a basis for the toxic nature of lead and the therapeutic properties of gold, respectively. Furthermore, both Pb(II) and Au(I) may modulate gene expression by selectively disrupting the function of ZF transcription factors [28, 29]. Consistent with the shared preference of copper and zinc for thiolate and amine coordination, Cu(II) is observed to displace Zn(II) from multiple ZF proteins, including the estrogen receptor and Fpg and XPA DNA repair proteins, resulting in loss of protein function [30–32]. Although Zn(II) ejection may result from oxidation of cysteine residues by Cu(II) to yield disulfide linked species, copper binding to the human estrogen receptor was confirmed via mass spectrometry and atomic absorption studies, indicating that copper can directly interact with Zn(II) binding sites under oxidizing conditions [33].

In contrast, although Cu(I) is the predominant form of copper in an intracellular environment, the ramifications of the thiophilic nature of both Zn(II) ions and Cu(I) ions have not been thoroughly studied. The presence of multiple CxxC repeats and additional thiolate ligands in ZF binding sites suggests the ability of Cu(I) to interact strongly with these motifs, as some natural copper binding sites that are built upon the CxxC motif exhibit binding constants on the order of 10^{17} – $10^{18} M^{-1}$ [34, 35]. Although Sommer et al. [36] showed that Cu(I) can replace Zn(II) from the ZF domains of *Chlamydomonas reinhardtii* copper response regulator 1, an SBP-domain transcription factor, Zn(II) displacement by Cu(I) did not appear to inhibit DNA binding. To our knowledge, no other studies regarding the impact of Cu(I) on ZF structure and function have been reported. Although all ZF domains feature a combination of cysteine and histidine residues as Zn(II) binding ligands, there is considerable structural diversity among the coordination motifs and resulting protein folds. Therefore, the susceptibility of Zn(II) to substitution by Cu(I) and the resulting impact on protein conformation deserves further study.

Given the diversity of Zn(II) binding motifs encountered in ZF domains, we chose to characterize the Cu(I) binding properties of ZF peptides featuring both different Zn(II) binding ligands and overall structural folds. Cu(I)-binding studies were conducted on the well-characterized consensus peptides CP-CCHH, CP-CCHC, and CP-CCCC, three peptides representative of the classical $\beta\beta\alpha$ ZF fold that differ only in their Zn(II) binding residues [18, 25, 37, 38]. The C-terminal ZF domain (residues 34–51) of nucleocapsid protein p7 (NCp7) of human immunodeficiency virus type 1 was also studied (referred to herein as NCp7_C). NCp7 is an RNA-binding protein that aids in the packaging of the viral genome and contains two copies of a ZF domain with the sequence Cys-X₂-Cys-X₄-His-X₄-Cys [39]. Although it

still maintains a CCHC metal binding site, the NCp7_C secondary structure on Zn(II) binding is more compact relative to the $\beta\beta\alpha$ fold exhibited by the consensus peptides, resulting in the term “zinc knuckle” often used to describe the structure of retroviral ZFs [40]. Moreover, the sequence contains a single tryptophan residue that serves as a fluorescent probe of the properly folded, Zn(II)-bound structure [41, 42]. Finally, both NCp7_C and the consensus peptide series exhibit high Zn(II) affinities, with apparent Zn(II) binding constants of 10^{12} – 10^{15} M $^{-1}$ [18, 38, 42, 43]. Taken together, the peptides studied here are suitable models for the study of the susceptibility of endogenous Zn(II) binding motifs toward Cu(I) substitution.

Materials and methods

Materials

Peptides were purchased from Genemed Synthesis or GenScript at more than 70 % purity and were further purified via reversed-phase high-performance liquid chromatography. Immediately prior to purification, peptides were incubated with 2 equiv of dithiothreitol per cysteine for 2 h at 55 °C to reduce all thiols. On purification, samples were immediately lyophilized to dryness and stored at -80 °C. All subsequent measurements were conducted in an anaerobic chamber (Coy Laboratory Products) maintained at 95 % N $_2$ /5 % H $_2$, unless otherwise stated. Peptide concentrations were calculated from the free thiol content determined by reaction with 5,5'-dithiobis(2-nitrobenzoic acid) (DTNB) to yield TNB $^{2-}$ ($\epsilon_{412\text{ nm}} = 14,150$ M $^{-1}$ cm $^{-1}$) [44]. The concentration of Co(II)-reconstituted peptide samples was calculated from measured extinction coefficients for $d-d$ transitions in the visible region of the spectrum (see the electronic supplementary material). Cu(I) stock solutions were prepared anaerobically by dissolving CuCl in 0.01 M HCl/1.0 M NaCl. The Cu(I) concentration was determined spectrophotometrically by addition of known amounts to excess bicinchoninate (BCA) to form Cu(BCA) $_2$ ($\epsilon_{562\text{ nm}} = 7,900$ M $^{-1}$ cm $^{-1}$) [45]. Zn(II) stock solutions were prepared by dilution of a zinc atomic absorption standard (15.29 mM in 2 % HNO $_3$). Co(II) solutions were prepared from a cobalt atomic absorption standard (17.0 mM in 2 % HNO $_3$) or by dissolution of CoCl $_2$ ·H $_2$ O in water. Co(II) concentrations of solutions made by the latter method were determined from the absorbance at 512 nm ($\epsilon_{512\text{ nm}} = 4.8$ M $^{-1}$ cm $^{-1}$) [25]. All buffers and stock solutions were prepared with Milli-Q purified water that had been passed over Chelex resin (Sigma) to remove trace metal ion contaminants.

Spectroscopic measurements

All measurements were made in either 50 or 200 mM *N*-(2-hydroxyethyl)piperazine-*N'*-ethanesulfonic acid, 100 mM NaCl at pH 7.5 unless otherwise noted. Absorption spectra were recorded with an Agilent 8453 spectrophotometer maintained inside the anaerobic chamber. To measure Cu(I) or Zn(II) binding to apo-peptides and Co(II)-reconstituted peptides, absorption spectra were recorded after the addition of 0.1 or 0.2 equiv of metal ion to 230 μ l of peptide in a small-volume quartz cuvette (Starna). Peptide concentrations ranged from 40 to 70 μ M. Samples were allowed to equilibrate between each addition of metal until no further spectral changes were observed (typically within 10 min). Care was taken to ensure that the total volume of added metal ion solution did not exceed 10 % of the initial volume. When the absorbance changes were plotted as a function of metal ion concentration, the concentrations of both the metal ion and the peptide were corrected for dilution. The spectrum of the corresponding apo-peptide was subtracted from all spectra resulting from the titration experiment.

Fluorescence spectra were recorded with a Varian Cary Eclipse spectrofluorimeter in septum-sealed quartz cuvettes. To study the impact of Zn(II) and Cu(I) on the intrinsic tryptophan fluorescence of NCp7_C, 3.5 μ M apo-NCp7_C (600 μ l) was prepared in a septum-sealed cuvette under anaerobic conditions. Emission spectra in the absence and presence of 1.1 equiv of Zn(II) were recorded from 300 to 450 nm on excitation at 280 nm. Cu(I) (0.2 equiv) was added via a gastight syringe, and emission spectra were recorded. To minimize fluorescence quenching owing to inner-filter effects, the optical density at 280 nm was less than 0.06 a.u. throughout the course of the experiment. Displacement of Zn(II) from NCp7_C by Cu(I) was monitored by using the Zn(II)-specific probe FluoZin-1 (Invitrogen). Six hundred microliter solutions of 10 μ M FluoZin-1, 25 μ M Zn(II), and 30 μ M NCp7_C were prepared in septum-sealed cuvettes under anaerobic conditions. The solutions were brought out of the glove box, and the fluorescence intensity at 520 nm was recorded on excitation at 495 nm. Cu(I) (1 or 2 equiv) was then added via a gastight syringe, and the fluorescence was recorded. Solutions of 10 μ M FluoZin-1 in the presence of Zn(II) and Cu(I) alone were also measured as controls.

Circular dichroism (CD) measurements were performed at 25 °C with an AVIV 215 CD spectrometer in a 1-mm cell. The samples were prepared in 10 mM tris(hydroxymethyl)aminomethane buffer, pH 7.5 to a final concentration of 40 μ M within a glove box (MBraun), and then sealed to retain an anaerobic environment during data collection. Six scans were averaged for each sample, and the buffer baseline was subtracted.

Results

Binding of Cu(I) to apo-ZF peptides

Cu(I) binding to the ZF apo-peptides under anaerobic conditions was monitored by measuring changes in the absorption spectrum in the ultraviolet region (Figs. 1, 2). For all peptides, addition of Cu(I) results in the appearance of an absorption feature centered at 263 nm with a shoulder at 300 nm, diagnostic of Cu(I)–thiolate charge transfer owing to cysteine coordination [46–48]. Previous studies of Cu(I) binding to metallothioneins yielded an absorption coefficient of approximately $5,300 \text{ M}^{-1} \text{ cm}^{-1}$ for single thiolate–Cu(I) bonds [49]. The molar extinction

NCp7_C: **KG****C****W****K****C****G****K****E****G****H****Q****M****K****D****C****T****E**
 CP-CCHH: **PYK****C****P****E****C****G****K****S****F****S****Q****K****S****D****L****V****K****H****Q****R****T****H****T****G**
 CP-CCHC: **PYK****C****P****E****C****G****K****S****F****S****Q****K****S****D****L****V****K****H****Q****R****T****C****T****G**
 CP-CCCC: **PYK****C****P****E****C****G****K****S****F****S****Q****K****S****D****L****V****K****C****Q****R****T****C****T****G**

Fig. 1 Sequence of the zinc finger peptides studied. Metal-binding residues are shown in red and bold, and the single tryptophan residue giving rise to intrinsic fluorescence is in blue

coefficients observed at 263 nm (approximately $10,000 \text{ M}^{-1} \text{ cm}^{-1}$; exact values are provided in the electronic supplementary material) for the complexes studied here exceed this value, suggesting that at least two cysteine thiols are involved in coordination.

The increase in absorbance as a function of the number of Cu(I) equivalents at multiple wavelengths indicates that the peptides bind multiple Cu(I) ions. For CP-CCHH, CP-CCHC, and NCp7_C, the absorbance at 263 nm increases until an approximately 1:1 Cu(I)-to-peptide ratio is achieved, whereas the absorbance at 242 nm continues to increase until a ratio of two Cu(I) ions per peptide. Increases in absorbance at all three wavelengths beyond 2 equiv of Cu(I) are attributed to Cu(I)–buffer interactions (confirmed by titration into buffer only; data not shown). Further increase at 242 nm beyond 1:1 stoichiometry could be owing to alteration of the Cu(I) coordination geometry at higher numbers of Cu(I) equivalents, and/or the formation of intermolecular interactions [48]. Cu(I) binding to CP-CCHH is distinctly biphasic for the addition of the first equivalent (see the electronic supplementary material). The molar extinction coefficient at 263 nm increases from $6,830 \pm 410$ to $11,420 \pm 1,180 \text{ M}^{-1} \text{ cm}^{-1}$, indicative of

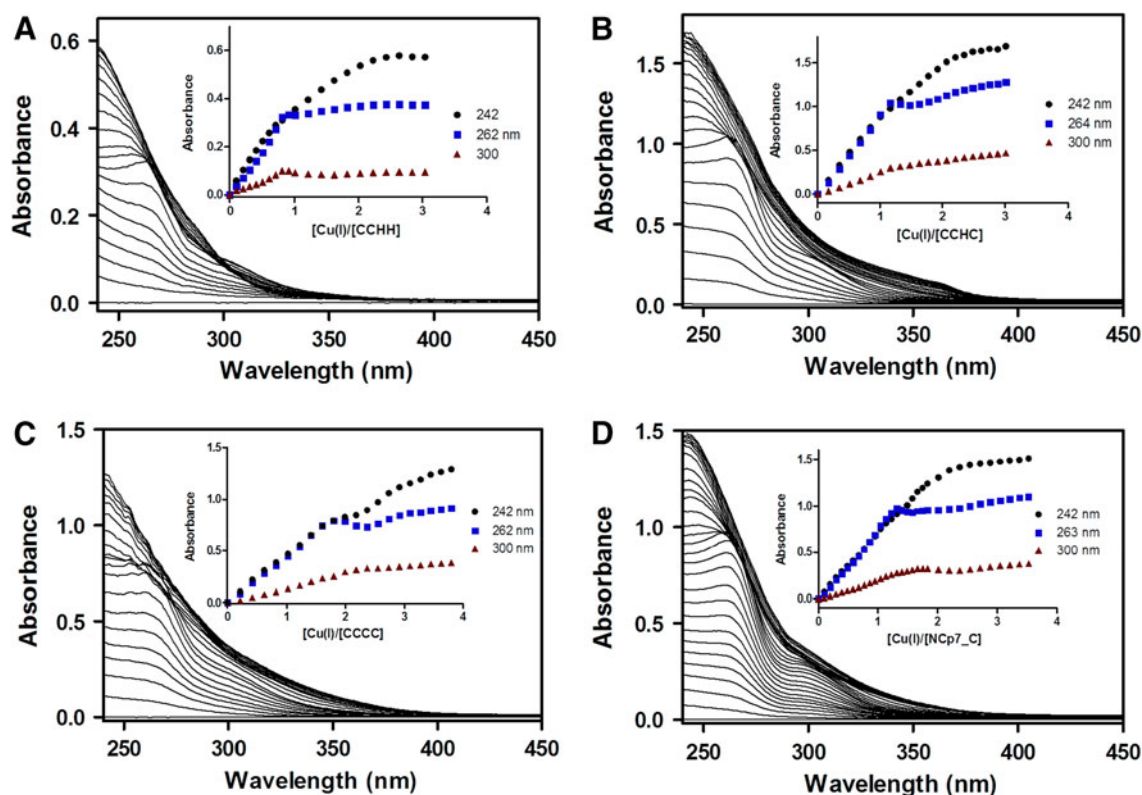


Fig. 2 Absorption spectra on the addition of Cu(I) to the apo-peptides: **a** CP-CCHH (50 μM), **b** CP-CCHC (84 μM), **c** CP-CCCC (50 μM), and **d** NCp7_C (74 μM). *Inset* increase in absorbance at 242 nm (circles), 263 nm (squares), and 300 nm (triangles) as a function of the number of Cu(I) equivalents added. The spectra were

recorded in 50 mM *N*-(2-hydroxyethyl)piperazine-*N'*-ethanesulfonic acid (HEPES), pH 7.5 and 100 mM NaCl. The spectrum of the apo-peptide was subtracted from each spectrum. The data are representative of three independent experiments

sequential formation of two distinct Cu(I)–thiolate species during this portion of the titration. One possible explanation for this observation is that the first 0.5 equiv of Cu(I) produces a dimeric peptide complex, and further addition of Cu(I) results in the formation of a different Cu(I) species with altered spectral properties. For CP-CCCC, formation of the Cu(I)–thiolate complex giving rise to the absorption feature at 262 nm persists well beyond a 1:1 stoichiometry, and substantial increases in absorbance at 242 nm continue beyond three Cu(I) ions per peptide. This greater Cu(I) binding stoichiometry likely reflects the higher thiol content of CP-CCC relative to the other peptides. Although the data do not rule out the formation of metal-bridged oligomers and/or heterogeneous complex formation, no precipitation was observed throughout the course of the titrations, suggesting the presence of nonspecific peptide aggregation is unlikely. Further investigation into the speciation of these complexes is ongoing.

Cu(I) substitution of cobalt–peptide complexes

To assess the ability of Cu(I) to bind to the ZF peptides in their metal-bound and properly folded form, we conducted absorption measurements in the presence of Co(II), which also forms tetrahedral complexes with mixed nitrogen/sulfur coordination sites. Although both Cu(I) and Zn(II) have d^{10} electronic configurations and are spectroscopically silent in the visible region, Co(II) exhibits distinct $d \rightarrow d$ transitions from 600 to 800 nm when bound to thiolate-rich sites and is commonly used as a spectroscopic probe for metal binding to ZF domains. The three consensus peptides and NCp7_C bind one Co(II) ion per ZF site with regular tetrahedral geometry around the Co(II) ions [18, 38, 41, 50]. Therefore, the resulting spectra are

diagnostic of the properly folded peptide and were used to monitor the binding of Zn(II) via competition experiments.

Addition of 1.1 equiv of Co(II) to the peptides results in distinguishing absorption features (Fig. 3, bold spectra) and extinction coefficients (see the electronic supplementary material) that are consistent with those previously reported for CP-CCHH, CP-CCHC, CP-CCCC, and NCp7_C. Absorption bands in the region from 250 to 400 nm are attributed to $S^- \rightarrow Co(II)$ charge transfer transitions, whereas those in the visible region represent $d-d$ electronic transitions. For all peptides, Co(II) binding was found to saturate at 75–80 % of the peptide concentration on the basis of the free thiol content determined via the DTNB assay (see “Materials and methods”). Metal-binding stoichiometries somewhat lower than 1 are not uncommon, given the susceptibility of cysteines to oxidation during peptide isolation [51].

Addition of Cu(I) to the Co(II)–peptide complexes results in a loss of absorption in the visible region in a concentration-dependent manner, consistent with displacement of Co(II) by Cu(I) at the metal binding site (Fig. 3). Moreover, the $S^- \rightarrow Co(II)$ charge transfer peaks in the ultraviolet region decrease in intensity, and a new peak at 263 nm grows in, corresponding with the Cu(I)–thiolate charge transfer transitions observed in Fig. 2 and providing evidence of Cu(I)–thiolate coordination at the Co(II) binding site. With the exception of CP-CCCC, the spectra exhibit tight isosbestic points, indicative of a transition from a single Co(II)-bound species to a Cu(I)-bound species without any intermediates. Shifting isosbestic points are observed in the earlier portions of the CP-CCCC titration, suggesting that multiple Cu(I)-bound species are formed. Additionally, both CP-CCHC and CP-CCCC exhibit curvature in the earlier portions of the

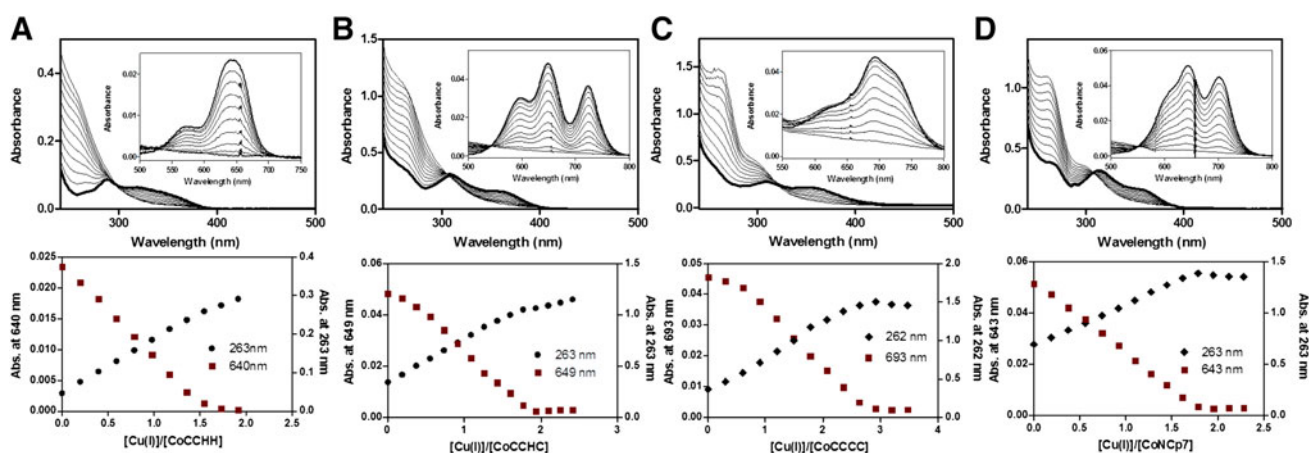


Fig. 3 *Top*: Absorption spectra on the addition of Cu(I) to the Co(II)-reconstituted peptides: **A** CoCP-CCHH (24.4 μ M), **B** CoCP-CCHC (59 μ M), **C** CoCP-CCCC (49 μ M), **D** CoNCp7_C (64 μ M). *Insets* absorption spectra of the visible region. *Bottom*: Change in

absorbance for both the visible Co(II) $d-d$ transitions (*squares*) and the copper–thiolate transition centered at 262 nm (*circles, diamonds*) for each peptide. The spectra were recorded in 200 mM HEPES, pH 7.5 and 100 mM NaCl

titration, indicative of cooperative binding until a critical concentration of Cu(I) occupancy has been reached.

Whereas complete Co(II) displacement with Zn(II) requires 1 equiv of metal for each Co(II)–peptide complex (see the electronic supplementary material), displacement by Cu(I) requires multiple ions per peptide. Complete displacement of Co(II) is observed on the addition of 1.5 equiv of Cu(I) to CoCP-CCHH. The nonintegral stoichiometry indicates that Cu(I) is likely inducing a multi-peptide complex in this case. Two Cu(I) ions are required to fully displace Co(II) from CoCP-CCHC and CoN-Cp7_C, whereas three ions are required for CoCP-CCCC, consistent with the formation of multinuclear Cu(I) complexes. Again, this difference in stoichiometry likely reflects the greater number of cysteine residues in CP-CCCC, leading to structures that accommodate a greater number of Cu(I) ions. Additionally, both CP-CCHC and CP-CCCC exhibit curvature in the earlier portions of the titration, indicative of a cooperative binding model in which binding of one Cu(I) ion results in an increase in the affinity for subsequent Cu(I) ions. Addition of Cu(I) to the Co(II)–peptide complexes produces an increase at 263 nm that persists through a higher metal-binding stoichiometry than that observed on titration of the apo-peptides, and the stoichiometry associated with the increase at 263 nm matches the stoichiometry for the loss of the Co(II) visible transitions. This observation indicates that the Cu(I) species formed on the addition of Cu(I) to the apo-peptides and those formed from displacement of Co(II) have different coordination environments with different spectral properties and/or are formed via different intermediates.

The lack of significant curvature near the titration end points for all peptides is evidence of complete or near-complete Co(II) displacement on the addition of each Cu(I) aliquot. Moreover, the shapes of the plots are independent of Co(II) concentration (up to 200-fold excess cobalt), indicating that even in the presence of excess Co(II), Cu(I) displacement is stoichiometric. On definitive characterization of the resulting Cu(I)-bound species, experiments will be initiated in the presence of appropriate chelators to determine Cu(I)-binding affinities. However, our current results indicate that Cu(I) binds to the peptides with an affinity that is orders of magnitude higher than that of Co(II). The similarity of the curve shapes observed on addition of Cu(I) to both CP-CCHC and NCp7_C shows that both complexes are equally susceptible to Co(II) displacement, and no impact of the nature of the secondary structure is apparent under these conditions. This is consistent with recent studies that show that Zn(II) affinity, and by analogy Co(II) affinity, is governed primarily by metal–ligand interactions, rather than protein stabilization via hydrophobic and/or hydrogen-bond interactions [51].

Displacement of Zn(II) from NCp7_C monitored via fluorescence spectroscopy

Co(II) exhibits substantially lower affinity for ZF domains than Zn(II). Specifically, recently Seneque and Latour [38] reported the Zn(II) affinities for CP-CCHH, CP-CCHC, and CP-CCCC to be approximately five orders of magnitude greater than those for Co(II). Therefore, to assess the susceptibility of the Zn(II)–peptide complexes to Cu(I) substitution, we monitored the impact of Cu(I) on Zn(II)NCp7_C via intrinsic peptide fluorescence from the tryptophan residue at position 37. Consistent with an earlier report, the fluorescence signal attributed to tryptophan increases considerably on the addition of Zn(II) (Fig. 4) [42]. Addition of Cu(I) to the Zn(II)-reconstituted peptide results in quenching of the tryptophan fluorescence, with complete quenching observed on the addition of 2 equiv of Cu(I). This binding stoichiometry matches that required for Co(II) displacement and reinforces the formation of a dinuclear Cu(I) species with NCp7_C. At the titration end point, the overall fluorescence is below that of the apo-peptide, indicative of a peptide configuration that is representative of neither the apo form nor the Zn(II)-bound form and/or quenching of tryptophan fluorescence by bound Cu(I). Even in the presence of 2 mM Zn(II), loss of fluorescence as a function of Cu(I) concentration is linear and exhibits a sharp end point, indicating that Cu(I) binds to NCp7_C at least 1.5 orders of magnitude more tightly than Zn(II) (see the electronic supplementary material).

Although the loss of Co(II)-specific absorption bands is strong evidence of Co(II) displacement, the loss of tryptophan fluorescence is less specific and could arise if Cu(I) binds away from the Zn(II) binding site and/or results in a complex with both bound Cu(I) and Zn(II) at the metal binding site. Moreover, the observation that fluorescence quenching by Cu(I) appears to be independent of Zn(II)

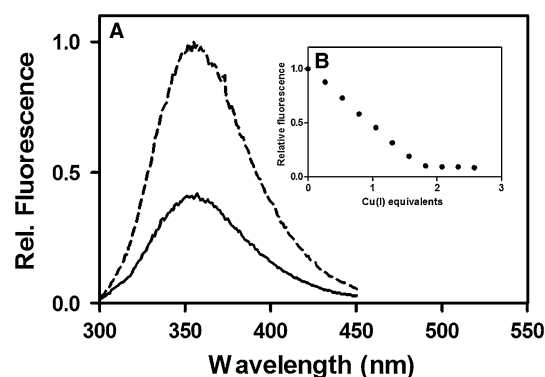


Fig. 4 Intrinsic fluorescence spectra ($\lambda_{\text{ex}} = 280 \text{ nm}$) of NCp7_C (3.75 μM) in the absence (solid line) and presence (broken line) of 5 μM Zn(II). *Inset* decrease in fluorescence intensity at 355 nm as a function of the number of equivalents of Cu(I) added

concentration within the range of 5–2,000 μM led us to directly probe for Zn(II) ejection on the addition of Cu(I). The Zn(II)-responsive probe FluoZin-1 was used to detect Zn(II) displaced from NCp7_C in the presence of Cu(I). Importantly, the affinities of both Zn(II) and Cu(I) for FluoZin-1 ($K_d = 30 \mu\text{M}$ and $K_d = 13 \mu\text{M}$, respectively; see the electronic supplementary material) are considerably less than those for NCp7_C, ensuring that the metal ions bind to NCp7_C preferentially. Moreover, the dye is far more responsive to Zn(II) than Cu(I).

In the presence of FluoZin-1, ZnNCp7_C results in little fluorescence at 520 nm relative to that observed in the presence of Zn(II) only, indicating that Zn(II) is fully bound by NCp7_C (Fig. 5). The addition of 1 equiv of Cu(I) results in the recovery of approximately half of the FluoZin-1 fluorescence, and 90 % of the fluorescence is recovered in the presence of 2 equiv of Cu(I). Moreover, the addition of copper results in far more fluorescence than predicted from the interaction of Cu(I) with FluoZin-1 at the same concentration, further evidence that Zn(II) is released from the peptide. Importantly, the observed concentration dependence of FluoZin-1 fluorescence recovery correlates with the 2:1 Cu(I)-to-NCp7_C stoichiometry observed on Co(II) displacement and Zn(II) displacement observed via tryptophan fluorescence. That full fluorescence recovery is not observed is likely due to the observed weak but nonnegligible affinity of FluoZin-1 for Cu(I), resulting in a slightly reduced fluorescence signal (see the electronic supplementary material). From this experiment, we conclude that the addition of Cu(I) results in Zn(II) ejection from NCp7_C, or at the very least results in the formation of a Zn(II)-bound complex that allows the dye to strip the Zn(II) from the binding pocket, despite the relatively low affinity of FluoZin-1 for Zn(II). Importantly, this assay is a generally applicable tool with which to directly probe for Zn(II) release on metal ion substitution, which is significant given the spectroscopically silent nature of Zn(II).

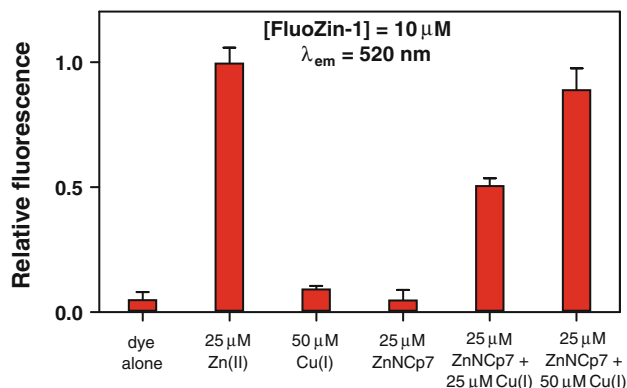


Fig. 5 Relative fluorescence of FluoZin-1 in the presence of the reagents indicated

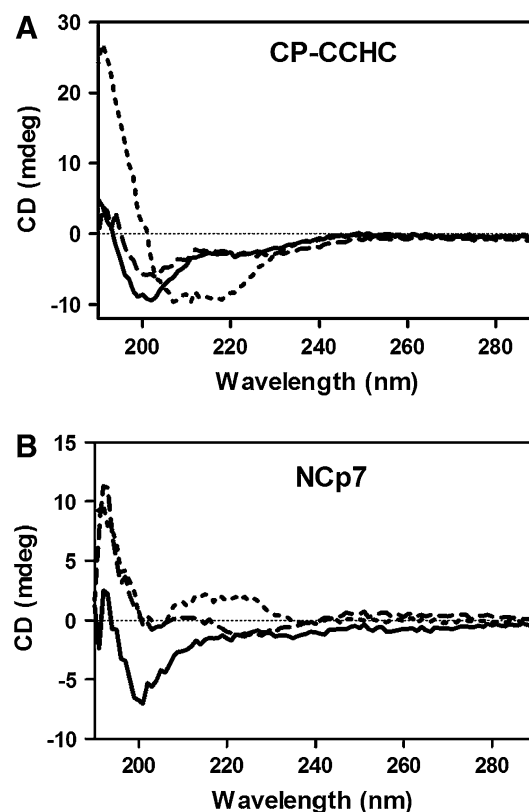


Fig. 6 Circular dichroism (CD) spectra recorded in 10 mM tris(hydroxymethyl)aminomethane pH 7.5 of apo (solid line), Zn(II) (short-dashed line), and Cu(I) (long-dashed line) CP-CCHC peptides (a) and NCp7_C peptides (b). The concentration of the peptide was 40 μM for all spectra

Impact of Cu(I) substitution on peptide structure

Given the greater binding stoichiometry observed for Cu(I) relative to Zn(II) and Co(II), it is probable that Cu(I) binding substantially alters the ZF structure, and likely, function. CD experiments were used to assess the impact of Cu(I) binding on the secondary structural fold of two sample peptides, CP-CCHC and NCp7_C. For both peptides, the spectra of the apo-peptides are characteristic of a random-coil conformation (Fig. 6). Addition of Zn(II) to CP-CCHC induces a strong maximum at 190 nm and a broad minimum at 210 nm, consistent with the $\beta\beta\alpha$ fold assumed by classical ZF peptides and spectra previously reported for CP-CCHC (Fig. 6a) [26, 38]. Addition of Cu(I) to CP-CCHC peptide, however, results in a spectrum similar to the random-coil spectrum of apo-CP-CCHC, indicating that no substantial secondary structure is induced in the presence of Cu(I). Similarly, the spectrum of Zn(II)NCp7_C features a broad maximum at 220 nm that reflects the defined peptide structure relative to the apo form [25]. In contrast, the Cu(I)NCp7_C spectrum resembles neither the apo complex nor the Zn(II)-reconstituted

complex, indicating that the structure differs significantly from either form (Fig. 6b). Overall, these spectra show that although the Cu(I) is strongly bound to these peptides, the properly folded structure of the ZF is lost on Cu(I) binding.

Discussion

To examine the susceptibility of endogenous Zn(II) binding sites toward Cu(I) substitution, we focused our studies on four ZF peptides. Our motivation to study ZFs is twofold:

1. ZF domains exhibit high metal binding affinity constants, making them relevant models with which to test the ability of Cu(I) ions to disrupt the complexes. Specifically, the consensus peptides studied here are reported to have apparent Zn(II) binding constants of 10^{15} M^{-1} , indicating that only metal ions which exhibit substantially strong thiol and/or histidine affinity will be able to displace Zn(II) [38].
2. Many ZF proteins function as transcription factors that control protein expression. The ability of Cu(I) to displace Zn(II) from ZF transcription factors, thereby altering the ZF function, could have a wide-ranging impact on the overall function of the organism, constituting a possible mechanism both for copper toxicity and copper-responsive ZF transcription factors.

The addition of Cu(I) to either Co(II)-reconstituted or Zn(II)-reconstituted ZF peptides results in rapid and complete substitution, identifying Cu(I) as the thermodynamically favored metal despite the known high affinity of ZF domains for both Co(II) and Zn(II). The peptides bind more than one Cu(I) ion per peptide, and the number of bound Cu(I) ions depends on the number of free cysteine thiols. CP-CCHC and NCp7_C, which exhibit different peptide folds in the presence of Zn(II), bind Cu(I) with the same stoichiometry and are equally susceptible to displacement of Co(II) by Cu(I). The nature of the secondary structure in the presence of Zn(II), and Co(II), does not appear to significantly impact the susceptibility of the peptides toward Cu(I) substitution for these two complexes.

ZF proteins exhibit tetrahedral geometry around the bound Zn(II) ion, whereas many Cu(I) metalloproteins that use thiol or thioether ligands exhibit mononuclear Cu(I) sites with coordination numbers of three or less [1, 14]. The ability of both CP-CCHC and NCp7_C to bind multiple Cu(I) ions at the Zn(II) binding site and the respective coordination geometry preferences for Zn(II) and Cu(I) suggest that the complexes should display different overall folds. Our CD results confirm this notion. The spectra of both Cu(I)-bound peptides differ

substantially from those of the Zn(II) complexes, confirming that the Zn(II)-induced secondary structure is lost on Cu(I) binding. Sommer et al. [36] reported that Cu(I) substitution at the ZF domains of the copper response regulator 1 transcription factor has no impact on the structure (as judged by CD) and DNA binding affinity, mandating that in this case Cu(I) is able to maintain the protein structure required for DNA interaction. Owing to the diversity in overall ZF structure and stability, the impact of Cu(I) substitution may not be universal. Furthermore, although ZF domains feature high-affinity sites, a wide range of Zn(II) affinity constants have been reported in the literature [38], suggesting that the susceptibility of ZF domains toward Cu(I) substitution will differ among ZFs as well as other zinc metalloproteins. Finally, it should be noted that the Cu(I)-binding behavior of synthetic peptides corresponding to isolated ZF domains may not directly reflect the binding properties of a larger protein construct and/or those of a protein–DNA complex. Experiments are being initiated to elucidate the impact of Cu(I) substitution on larger ZF proteins in both the absence and the presence of cognate DNA.

Functional copper homeostasis in eukaryotic cells results in vanishingly low levels of “free,” unbound Cu(I) [52], raising the question of how ZF domains would acquire copper in vivo. Under conditions of copper accumulation, copper is stored in a redox-inactive form on complex formation with metallothioneins, cysteine rich proteins that also bind Zn(II) and Cd(II) [53]. In principle, copper under these conditions could transfer from Cu(I)-bound metallothioneins and/or Cu(I)-bound glutathione to Zn(II)-bound ZF complexes and/or newly synthesized apoproteins. The relative Cu(I) affinities of Cu(I)-binding biomolecules and ZFs are needed to address the possibility of Cu(I) transfer from biologically relevant Cu(I) complexes. Recent imaging experiments of intracellular copper levels show that calcium release in neuronal cells triggers a redistribution of mobile copper pools, suggesting that copper may play a role in cellular signaling [54]. Although the experiments could not differentiate between free and bound, yet mobile, copper pools owing to the strong affinity of the fluorescent chelator used, the potential for copper signaling raises several new questions regarding the dynamics of copper homeostasis, one of which is the ligated state of copper during such signaling events. Finally, several neurodegenerative diseases, including Alzheimers, Parkinson's, and prion diseases, are associated with misregulated copper homeostasis. Although the involvement of copper in the pathogenesis of these diseases is not well understood, the observed changes in copper metabolism within the brain may allow transiently elevated cellular copper levels, thereby promoting promiscuous copper binding.

In addition to providing deleterious reactions under copper-replete conditions, the high affinity of Cu(I) for Zn(II) binding domains might serve as a molecular basis for copper sensing. In *Enterococcus hirae*, the *cop* operon regulates copper uptake, availability, and export. The transcriptional repressor CopY has a CxCxxxCxC motif that, when bound to Zn(II), stabilizes binding of CopY to promoter DNA. As the level of ambient copper rises, the Atx1-like copper chaperone CopZ delivers two Cu(I) ions to CopY, resulting in Zn(II) displacement, dissociation of CopY from the promoter, and induction of the *cop* operon [55, 56]. Although no affinity constants have been reported, the capability of Cu(I) to displace Zn(II) from a Cys₄ binding site suggests that the reversibility and moderate affinity of protein–Zn(II) interactions might provide a basis for intracellular metal sensing. Similarly, the ZF domain of the Sp1 transcription factor functions as a sensor of copper that regulates hCtr1 (the primary mammalian copper uptake protein) levels in response to changing copper concentrations [57]. One could hypothesize that Cu(I) displacement at the Zn(II) binding site promotes a structural change in Sp1 that allows differential expression of hCtr1 in the presence of different copper concentrations. Given the diversity of structure and function of ZF domains, the impact of Cu(I) on the structure and function of other endogenous Zn(II) binding domains deserves further study.

Acknowledgments This work was supported by a Research Corporation Cottrell College Award (no. 7862 to K.E.S.), Macalester College, and Santa Clara University. We thank Robert Rossi of Macalester College for assistance with electronic absorption experiments and Daryl Eggers of San Jose University for use of his CD spectrometer.

References

- Boal AK, Rosenzweig AC (2009) Chem Rev 109:4760–4779
- Robinson NJ, Winge DR (2010) Annu Rev Biochem 79:537–562
- Kaplan JH, Lutsenko S (2009) J Biol Chem 284:25461–25465
- Halliwell B, Gutteridge JMC (1990) Methods Enzymol 186:1–85
- Macomber L, Rensing C, Imlay JA (2007) J Bacteriol 189:1616–1626
- Adlard PA, Bush AI (2006) J Alzheimers Dis 10:145–163
- Gaggelli E, Kozlowski H, Valensin D, Valensin G (2006) Chem Rev 106:1995–2044
- Brown DR (2009) Dalton Trans 4069–4076
- Macomber L, Imlay JA (2009) Proc Natl Acad Sci USA 106:8344–8349
- Totter S, Patterson CJ, Banci L, Bertini I, Felli IC, Pavelkova A, Dainty SJ, Pernil R, Waldron KJ, Foster AW, Robinson NJ (2012) Proc Natl Acad Sci USA 109:95–100
- Berg JM, Shi Y (1996) Science 271:1081–1085
- Berg JM, Godwin HA (1997) Annu Rev Biophys Biomol Struct 26:357–371
- Krishna SS, Majumdar I, Grishin NV (2003) Nucleic Acids Res 31:532–550
- Laity JH, Lee BM, Wright PE (2001) Curr Opin Struct Biol 11:39–46
- Andreini C, Banci L, Bertini I, Rosato A (2006) J Proteome Res 5:196–201
- diTargiani RC, Lee SJ, Wassink S, Michel SL (2006) Biochemistry 45:13641–13649
- Krizek BA, Berg JM (1992) J Am Chem Soc 114:2984–2986
- Krizek BA, Merkle DL, Berg JM (1993) Inorg Chem 32:937–940
- Michalek JL, Lee SJ, Michel SLJ (2012) J Inorg Biochem 112:32–38
- Bal W, Schwerdtle T, Hartwig A (2003) Chem Res Toxicol 16:242–248
- Lai Z, Freedman DA, Levine AJ, McLendon GL (1998) Biochemistry 37:17005–17015
- Payne JC, Rous BW, Tenderholt AL, Godwin HA (2003) Biochemistry 42:14214–14224
- Roehm PC, Berg JM (1997) Biochemistry 36:10240–10245
- Ghering AB, Jenkins LM, Schenck BL, Deo S, Mayer RA, Pikaart MJ, Omichinski JG, Godwin HA (2005) J Am Chem Soc 127:3751–3759
- Payne JC, Horst MAt, Godwin HA (1999) J Am Chem Soc 121:6850–6855
- Franzman MA, Barrios AM (2008) Inorg Chem 47:3928–3930
- Larabee JL, Hocker JR, Hanas JS (2005) Chem Res Toxicol 18:1943–1954
- Handel ML, deFazio A, Watts CK, Day RO, Sutherland RL (1991) Mol Pharmacol 40:613–618
- Zawia NH, Sharan R, Brydie M, Oyama T, Crumpton T (1998) Dev Brain Res 107:291–298
- Asmuss M, Mullenders LH, Eker A, Hartwig A (2000) Carcinogenesis 21:2097–2104
- Hartwig A, Asmuss M, Ehleben I, Herzer U, Kostelac D, Pelzer A, Schwerdtle T, Burkle A (2002) Environ Health Perspect 110(Suppl 5):797–799
- Predki PF, Sarkar B (1992) J Biol Chem 267:5842–5846
- Hutchens TW, Allen MA, Li CM, Yip T-T (1992) FEBS Lett 309:170–174
- Badarau A, Dennison C (2011) Proc Natl Acad Sci USA 108:13007–13012
- Xiao ZG, Brose J, Schimo S, Ackland SM, La Fontaine S, Wedd AG (2011) J Biol Chem 286:11047–11055
- Sommer F, Kropat J, Malasarn D, Grosseohme NE, Chen XH, Giedroc DP, Merchant SS (2010) Plant Cell 22:4098–4113
- Krizek BA, Amann BT, Kilfoil VJ, Merkle DL, Berg JM (1991) J Am Chem Soc 113:4518–4523
- Seneque O, Latour JM (2010) J Am Chem Soc 132:17760–17774
- Darlix JL, Lapadattapolsky M, Derocquigny H, Roques BP (1995) J Mol Biol 254:523–537
- South TL, Blake PR, Hare DR, Summers MF (1991) Biochemistry 30:6342–6349
- Bombarda E, Cherradi H, Morellet N, Roques BP, Mely Y (2002) Biochemistry 41:4312–4320
- Mely Y, De Rocquigny H, Morellet N, Roques BP, Gerad D (1996) Biochemistry 35:5175–5182
- Magyar JS, Godwin HA (2003) Anal Biochem 320:39–54
- Riddles PW, Blakeley RL, Zerner B (1983) Methods Enzymol 91:49–60
- Xiao ZG, Loughlin F, George GN, Howlett GJ, Wedd AG (2004) J Am Chem Soc 126:3081–3090
- Rousselot-Pailley P, Seneque O, Lebrun C, Crouzy S, Boturny D, Dumy P, Ferrand M, Delangle P (2006) Inorg Chem 45:5510–5520
- Liu T, Ramesh A, Ma Z, Ward SK, Zhang L, George GN, Talaat AM, Sacchettini JC, Giedroc DP (2007) Nat Chem Biol 3:60–68
- Angeletti B, Waldron KJ, Freeman KB, Bawagan H, Hussain I, Miller CC, Lau KF, Tennant ME, Dennison C, Robinson NJ, Dingwall C (2005) J Biol Chem 280:17930–17937

49. Pountney DL, Schauwecker I, Zarn J, Vasak M (1994) *Biochemistry* 33:9699–9705
50. Fitzgerald DW, Coleman JE (1991) *Biochemistry* 30:5195–5201
51. Rich AM, Bombarda E, Schenk AD, Lee PE, Cox EH, Spuches AM, Hudson LD, Kieffer B, Wilcox DE (2012) *J Am Chem Soc* 134:10405–10418
52. Rae TD, Schmidt PJ, Pufahl RA, Culotta VC, O'Halloran TV (1999) *Science* 284:805–808
53. Sutherland DEK, Stillman MJ (2011) *Metallomics* 3:444–463
54. Dodani SC, Domaille DW, Nam CI, Miller EW, Finney LA, Vogt S, Chang CJ (2011) *Proc Natl Acad Sci USA* 108:5980–5985
55. Cobine PA, George GN, Jones CE, Wickramasinghe WA, Solioz M, Dameron CT (2002) *Biochemistry* 41:5822–5829
56. Cobine PA, Jones CE, Dameron CT (2002) *J Inorg Biochem* 88:192–196
57. Song IS, Chen HHW, Aiba I, Hossain A, Liang ZD, Klomp LWJ, Kuo MT (2008) *Mol Pharmacol* 74:705–713